We have measured the transverse relaxation time, T_{2C}, for the major features in the spectrum of the same dried sample of microcrystalline cellulose. This measurement involves a modification[7] of the original echo sequence discussed by Hahn.[10] Figure 1 includes the values obtained for the T_{2C} values, reported as effective full widths at half-maximum, $\Delta\nu(T_{2C}) = (\pi T_{2C})^{-1}$. The estimated errors in $\Delta\nu(T_{2C})$ are ± 2 Hz. Most of these relaxation data were nominally exponential; the decay for C-6 was clearly nonexponential and could be decomposed into two components having associated line widths of 14 and 4 Hz. The faster relaxing component was identified to be the upfield tail of the resonance line.

These relaxation studies permit several qualitative conclusions regarding the structure of cellulose I. The T_{1C} values observed and presumably the molecular motions are in a range between those observed in glassy synthetic polymers and highly crystalline materials.[11] We cannot exclude the possibility that the relaxation is due to motion of water molecules that remain after the drying process or motion of labile protons. Both the T_{1C} and T_{2C} data show a faster relaxation for the carbons in the upfield tail of C-6 relative to the sharp peak. This suggests a greater mobility or more access to labile protons for those carbons in the tail as opposed to the sharp peak of C-6. The corresponding chemical shift may arise from differences in conformation, hydrogen bonding, or crystal packing.

The observed full widths at half height, $\Delta\nu^*$, in the CP MASS spectrum of cellulose I range from 30 to 85 Hz. This can be constrasted with measured $\Delta\nu(T_{2C})$ values of <5 Hz. Since the instrumental broadening is estimated to be <3 Hz, the majority of the $\Delta\nu^*$ is attributed to a dispersion of chemical shifts along with smaller magnetic susceptibility contributions which survive the sample spinning. For comparison, the line widths obtained from a crystalline sample of glucose are <11 Hz. The chemical shift dispersions observed in cellulose I are probably due to irregularities in crystal packing which distort the glucose monomer or change the hydrogen bonding and produce slightly different shifts for different monomers.

From a magnetic resonance point of view, the coarser chemical shift features exemplified by the splitting of C-4 into two separate resonances, the shoulder associated with C-6 and the incipient splitting of the resonance of C-1 into two peaks of nearly equal intensity (in spectra of celluloses derived from cotton an actual splitting is barely resolved) all indicate that the glucose units are found in two magnetically inequivalent environments in dry cellulose I. The resulting picture that one obtains is that the glucose monomers in cellulose are rather rigidly fixed in position but that the crystalline packing is not nearly as regular as one would observe in a crystalline molecular solid or even a highly crystalline synthetic polymer such as polyethylene. It also appears that there exist two types of glucose monomers, one of which allows more freedom of motion or access to labile protons for the pendant C-6. It is not clear what the morphology of these "free C-6's" is, but it is possible that they are in amorphous regions or simply on the outer faces of the elementary fibrils[12] of cellulose. If one interprets the broad peak at 85 ppm to be due to C-4 carbons which are in amorphous regions of the polymer, the relaxation data indicates that the main chain in these amorphous regions does *not* have significantly more motional freedom than those glucose units in the crystalline portion of the sample. Alternatively, if the peak at 85 ppm is due to glucose units on the surface of the elementary fibrils and that at 90 ppm is due to glucose units buried in the center of the elementary fibril or vice-versa, then differences in hydrogen bonding or bond angles will likely be present to account for the observed chemical shifts.

We have measured CP MASS spectra of several different preparations of cellulose and are beginning relaxation studies of these samples. It is hoped that by integrating all of this information we will be able to arrive at a consistent picture of cellulose structure and its relationship to the NMR spectra obtained. It is clear that cellulose is a complicated system and that unambiguous information comes only with the greatest difficulty.

References and Notes

(1) After this work was in progress, we were informed of similar research by Atalla, Gast, Sindorf, Bartuska, and Maciel (see preceding paper in this issue) concerning the solid state NMR of cellulose. We would like to thank those authors for cordial exchange of information so that not too much effort would be duplicated.
(2) Schaefer, J.; Stejskal, E. O.; Buchdahl, R. *Macromolecules* **1977**, *10*, 384–405.
(3) Pines, A.; Gibby, M. G.; Waugh, J. S. *J. Chem. Phys.* **1973**, *59*, 569–590.
(4) Andrew, E. R.; Bradbury, A.; Eades, R. G. *Nature (London)* **1958**, *182*, 1659. Lowe, I. J. *Phys. Rev. Lett.* **1959**, *2*, 285–287.
(5) Pfeffer, P. E.; Valentine, K. M.; Parrish, R. W. *J. Am. Chem. Soc.* **1979**, *101*, 1265–1275, and references therein.
(6) Sigmacel, Type 50, Microcrystalline Cellulose, Sigma Chemical Co.
(7) Earl, W. L.; Vanderhart, D. L. *Macromolecules* **1979**, *12*, 762–767.
(8) Vanderhart, D. L., unpublished work.
(9) See, for example, Farrar, T. C.; Becker, E. D. "Pulse and Fourier Transform NMR"; Academic Press: New York, 1971; p 22.
(10) Hahn, E. L. *Phys. Rev.* **1950**, *80*, 580–594.
(11) Schaefer, J.; Stejskal, E. O.; Buchdahl, R. *Macromolecules* **1975**, *8*, 291–296.
(12) Blackwell, J.; Kolpak, F. J. *Macromolecules* **1975**, *8*, 322–326.

William L. Earl
Center for Fire Research
National Bureau of Standards, Washington, D.C. 20234

D. L. VanderHart*
Center for Materials Science
National Bureau of Standards, Washington, D.C. 20234

Received October 9, 1979

Detection of "Tension" and Electronic Asymmetry in Imidazole-Appended Iron Porphyrins by NMR Spectroscopy

Sir:

Imidazole-appended iron porphyrins have played an important role in understanding the fundamental chemistry of hemoglobin and myoglobin oxygen binding.[1-4] Such covalently linked models will likely contribute toward elucidation of structure and mechanism in other classes of hemoproteins.[5,6] The first reported and most intensively investigated compounds are based on an amide linkage to a propionic acid side chain of natural-derivative porphyrins.[1,2] Traylor and co-workers have recently demonstrated that such models may simulate the oxygen binding kinetics and thermodynamics, as well as imidazole "tension" effects presumably responsible for the allosteric trigger in hemoglobin.[1] Collman et al. likewise utilized the "picket fence" iron porphyrin and an imidazole-appended analogue to illustrate the sensitivity of oxygen binding thermodynamics to the steric nature of the trans-coordinated imidazole ligand.[3] Additional imidazole-appended tetraphenylporphyrin (TPP) derivatives have recently been prepared via amide linkage to a single aminophenyl group[6,7] or to a pyrrole side-chain residue.[8]

A TPP-appended derivative has been prepared in this laboratory by an alternate synthetic route. An ether linkage is readily formed between the functionalized TPP species, 5-(2-hydroxyphenyl)-10,15,20-tritolylporphyrin, and a dibromoalkane.[9] The isolated bromoalkoxy porphyrin is allowed to react with imidazole using DMF solvent in the presence of a suitable base (K_2CO_3 or triethylamine). Iron insertion and subsequent chromatographic purification yields a product consistent with the structure shown in Figure 1 [isolated as the

0002-7863/80/1502-3252$01.00/0

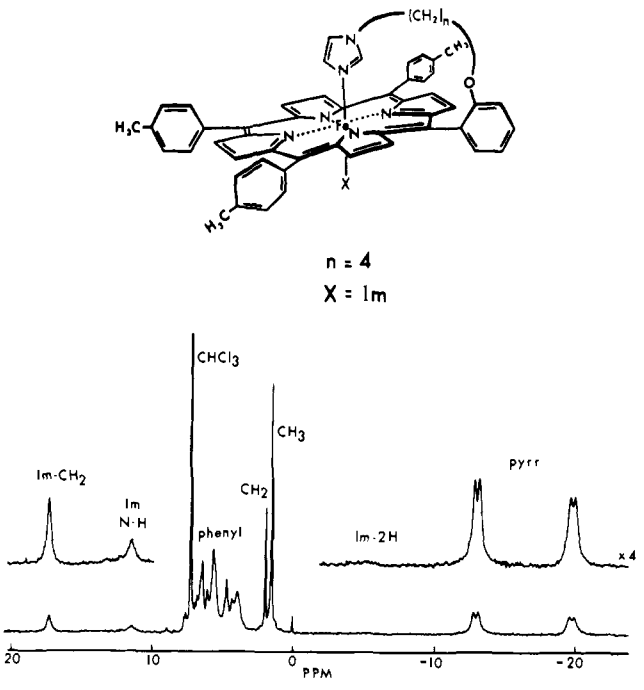

Figure 1. ^{1}H NMR spectrum of *N*-butylimidazole-appended iron(III) tetraphenylporphyrin derivative: iron porphyrin, 0.02 M; imidazole, 0.022 M; $CDCl_3$ solvent; 26 °C.

iron(III) chloride].[10] Rationale for physical examination of this new appended iron porphyrin vs. natural-porphyrin derivatives is found in the C_s molecular symmetry and product homogeneity. On the other hand, coupling an imidazole function at either the 6- or 7-position propionic acid of a natural porphyrin yields two linkage isomers. Two additional coordination isomers are present as a consequence of total asymmetry in porphyrin ring substitution.

^{1}H NMR examination of the new imidazole-appended iron (III) porphyrin chloride derivatives reveals a nearly equal mixture of high-spin and low-spin species[11] presumably as a result of both intra- and intermolecular coordination (at 0.01 M). Formation of the bis-ligated low-spin iron(III) state is favored at the expense of intramolecular coordination in part of the molecules. Variable-temperature measurements show no change in the ratio of high-spin to low-spin species, thus indicating no evidence for a spin equilibrium process. Acid-base titration reveals reversible imidazole protonation and displacement as a ligand. Imidazole titration yields a new, entirely low-spin complex with distinctive NMR peaks[11] upon addition of 1 mol equiv of exogenous ligand (Figure 1).

Figure 2 summarizes upfield pyrrole ^{1}H NMR resonances for imidazole-appended and related complexes. In Figures 2a-d the character of the axial ligand has been held constant in the form of *N*-alkylimidazole residues. Introduction of a single phenyl *o*-$OCH_2CH_2CH_3$ group into the TPP structure induces considerable asymmetry in the NMR isotropic shift pattern (Figure 2c) yielding four sets of pyrrole proton signals. This electronic asymmetry is modified for imidazole-appended complexes (Figures 2a and 2b). Molecular models suggest decreased conformational freedom in complexes formed with the propylimidazole appendage compared with that in the butyl analogue. Accordingly, the varying shift and splitting patterns in Figure 2 may be ascribed to "tension" in the form of tilting or elongation of the imidazole-iron bond. The nonappended, but electronically equivalent, complex in Figure 2c must then represent the totally "relaxed" state. Extreme electronic asymmetry is apparent in Figure 2e when 2-methylimidazole is employed as a second ligand in the appended complex. The 2-methyl group must sterically interact with the porphyrin to

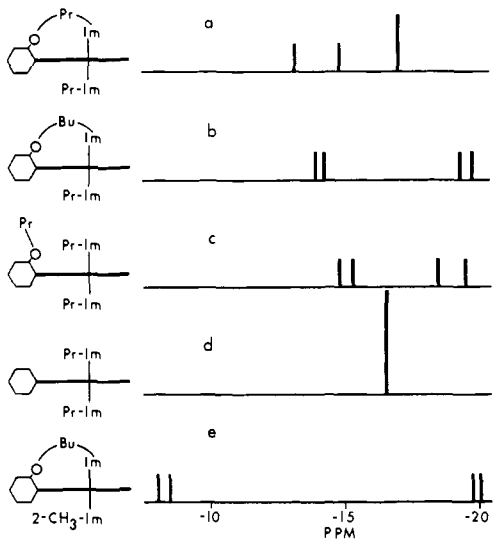

Figure 2. Upfield pyrrole ^{1}H NMR resonances of iron(III) tetraphenylporphyrin derivatives: iron porphyrin complexes, ~0.02 M; $CDCl_3$ solvent; 26 °C.

yield a strained linkage which serves to magnify bonding constraints imposed by the *trans*-imidazole appendage. Considerably smaller asymmetry effects are observed when cyanide is employed as the exogenous ligand. Likewise, differences are seen in the spread of pyrrole protons for high-spin iron(II) complexes, but interpretation is complicated by necessary use of the sterically constrained 2-methylimidazole ligand[13] to generate the nonappended species.

The mechanism of unpaired spin rearrangement among complexes in Figure 2 is speculative. Lifting of orbital degeneracy with consequent rhombic magnetic anisotropy would induce in-plane dipolar shifts varying in sign around the ring.[14] However, this mechanism for increasing the spread of pyrrole resonances does not appear to be predominant as no large differences are observed in the spread of phenyl resonances for the various complexes. Differences in contact spin density at the four pyrrole groups through perturbation of π symmetry appears more likely, as line widths (from contact relaxation) of pyrrole signals in Figure 1 are a function of shift magnitude.[15]

Shift patterns for ring methyl protons among various low-spin ferric hemoproteins are known to show large differences.[16] In addition, the pattern of signals always differs for the hemoprotein vs. the isolated iron porphyrin complex.[15,16] In this regard the imidazole-appended complexes appear to model variations in electronic asymmetry apparent for hemoproteins. La Mar et al. have demonstrated the importance of peripheral porphyrin-protein contacts in determining the relative spread of ring methyl resonances.[15] However, an additional contribution from constraints placed on imidazole bonding or orientation appears reasonable, and is supported by examination of the appended models. In studies concurrent with this one, Walker[7] and Traylor et al.[17] have emphasized orientation of the imidazole plane as a factor in determining asymmetry of unpaired spin delocalization. Whatever the nature of the symmetry-breaking mechanism in imidazole-appended iron porphyrins, the possibility must now be considered that axial imidazole "tension" is of general importance in dictating electronic, spectroscopic, and chemical properties of hemoproteins.

Acknowledgments. Acknowledgment is made to donors of the Petroleum Research Fund, administered by the American Chemical Society, for partial support of this research. Support from the Research Corporation is also gratefully acknowledged.

References and Notes

(1) Geibel, J.; Cannon, J.; Campbell, D.; Traylor, T. G. *J. Am. Chem. Soc.* **1978**, *100*, 3575–3585, and references contained therein.
(2) Sharma, V. S.; Geibel, J. F.; Ranney, H. M. *Proc. Natl. Acad. Sci. U.S.A.* **1978**, *75*, 3747–3750.
(3) Collman, J. P.; Brauman, J. I.; Doxsee, K. M.; Halbert, T. R.; Suslick, K. S. *Proc. Natl. Acad. Sci. U.S.A.* **1978**, *75*, 564–568.
(4) Reed, C. A. In "Metal Ions in Biological Systems", Sigel, H., Ed.; Marcel Dekker: New York, 1978; Vol 7, Chapter 7.
(5) Goff, H.; Morgan, L. O. *Inorg. Chem.* **1976**, *15*, 2062–2068.
(6) Mashiko, T.; Marchon, J.-C.; Musser, D. T.; Reed, C. A.; Kastner, M. E.; Scheidt, W. R. *J. Am. Chem. Soc.* **1979**, *101*, 3653–3655.
(7) (a) Walker, F. A.; Benson, M. E. Abstracts of Papers, ACS/CSJ Chemical Congress, Honolulu, Hawaii, April 1–6, 1979; American Chemical Society: Washington, D.C., 1979; INOR 309. (b) See Walker, F. A. *J. Am. Chem. Soc.*, following paper in this issue.
(8) (a) Momenteau, M.; Loock, B.; Bisagni, E.; Rougee, M. *Can. J. Chem.* **1979**, *57*, 1804–1813. (b) Lavalette, D.; Tetreau, C.; Momenteau, M. *J. Am. Chem. Soc.* **1979**, *101*, 5395–5401.
(9) (a) Little, R. G.; Anton, J. A.; Loach, P. A.; Ibers, J. A. *J. Heterocycl. Chem.* **1975**, *12*, 343–349. (b) Little, R. G. *Ibid.* **1978**, *15*, 203–208.
(10) Products were shown to be homogeneous on silica gel thin layer chromatography. ^1H and ^{13}C NMR spectroscopy of metal-free porphyrin and iron(III) imidazole derivatives was consistent with expected structures.
(11) Resonance assignments are readily made based on earlier literature studies of high-spin and low-spin iron(III) porphyrins.[12]
(12) (a) Walker, F. A.; La Mar, G. N. *Ann. N.Y. Acad. Sci.* **1973**, *206*, 328–348. (b) Satterlee, J. D.; La Mar, G. N. *J. Am. Chem. Soc.* **1976**, *98*, 2804–2808.
(13) Goff, H.; La Mar, G. N.; Reed, C. A. *J. Am. Chem. Soc.* **1977**, *99*, 3641–3646.
(14) Shulman, R. G.; Glarum, S. H., Karplus, M. *J. Mol. Biol.* **1971**, *57*, 93–115.
(15) La Mar, G. N.; Viscio, D. B.; Smith, K. M.; Caughey, W. S.; Smith, M. L. *J. Am. Chem. Soc.* **1978**, *100*, 8085–8092.
(16) (a) Phillips, W. D. In "NMR of Paramagnetic Molecules", La Mar, G. N., Horrocks, W. DeW., Jr., Holm, R. H., Eds.; Academic Press: New York, 1973; Chapter 11. (b) Morrow, J. S.; Gurd, F. R. N. *CRC Crit. Rev. Biochem.* **1975**, *3*, 221–287.
(17) Traylor, T. G.; Chang, C. K.; Geibel, J.; Berzinis, A.; Mincey, T.; Cannon, J. *J. Am. Chem. Soc.* **1979**, *101*, 6716–6731.

Harold Goff

Department of Chemistry, University of Iowa, Iowa City, Iowa 52242

Received October 22, 1979

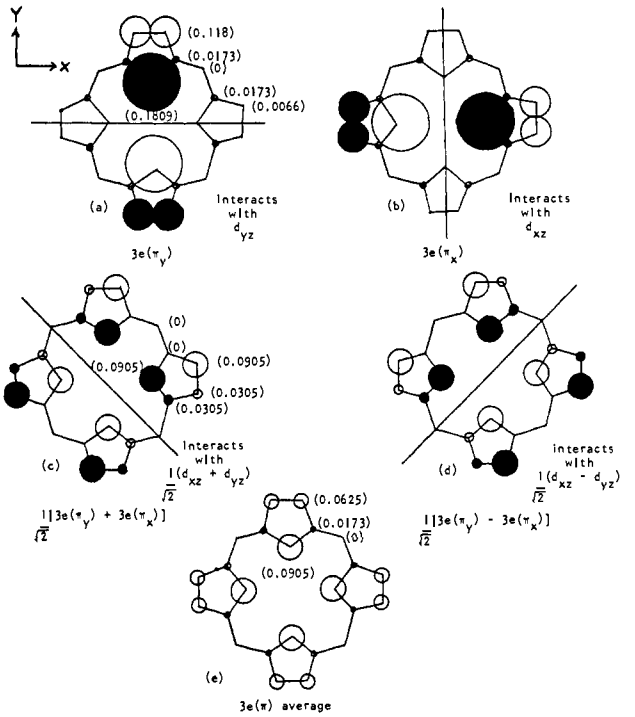

Figure 1. (a, b) Electron density and nodal properties of porphine $3e(\pi)$ orbitals,[10] which interact with the d_{xz} and d_{yz} orbitals of low-spin Fe(III), respectively. (c, d) Linear combinations of these orbitals, appropriate for interaction with meso-bonded planar ligands. (e) Average electron density distribution if the $3e(\pi)$ orbitals remain degenerate. The light and dark shades depict orbital symmetry properties, and the numbers in parentheses give the square of the atomic orbital mixing coefficients, c_i^2, for each position. These c_i^2 values are proportional to the unpaired electron density, ρ_i, expected at the carbon i. The size of the circles depicts the relative size of c_i^2.

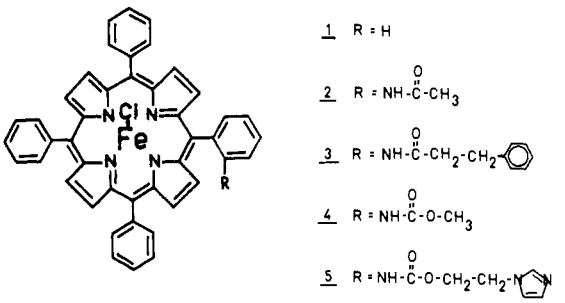

Figure 2. Structures of the iron porphyrins used in this study.

Models of the Cytochromes *b*. 1. Effect of Substituents, Axial Ligand Plane Orientation, and Possible Axial Ligand Bond Strain on the Pyrrole Proton Shifts of a Series of Low-Spin Monosubstituted Tetraphenylporphinatoiron(III)–Bisimidazole Complexes

Sir:

The factors affecting the magnitude of contact shifts of low-spin iron(III) porphyrins in high-symmetry synthetic compounds,[1,2] simple natural hemins,[1,3] and hemoproteins[4–9] have been investigated in detail for some time. In particular, attempts have been made to explain the variation in the position of the methyl resonances of iron(III) protoporphyrin containing hemoproteins.[1,3–9] Since the contact shift pattern of low-spin iron(III) porphyrins indicates spin delocalization mainly to the pyrrole positions,[1,2] involvement of the porphyrin $3e(\pi)$ orbitals[10] in ligand-to-metal π-back-bonding to the remaining hole in the d_{xz}, d_{yz} orbitals of iron has been postulated as the mechanism of unpaired spin delocalization for both synthetic and natural low-spin iron(III) porphyrins.[1–3]

One hypothesis[1,5] which may explain the variation in methyl contact shifts is that planar axial ligand(s) split the degeneracy of the $3e(\pi)$ filled molecular orbitals of the porphyrin ring and the *e*-symmetry d_{xz}, d_{yz} orbitals of the metal; thus unpaired electron delocalization to certain pyrrole positions is favored over others. This situation is explained more clearly by reference to Figure 1, in which the electron densities and nodal properties of the $3e(\pi)$ orbitals[10] of porphine are presented. Although the energies of d_{xz} and d_{yz} are expected to be split by the dynamic Jahn-Teller effect,[5] the electron populations of the two d orbitals appear to be equal at room temperature, in the absence of symmetry-breaking effects. Such is the case for low-spin tetraphenylporphyrin, octaethylporphyrin, and *meso*-tetra-*n*-propylporphyrin complexes of iron(III), all of which have fourfold molecular symmetry because the axial ligands rotate freely about the metal-ligand bonds. All of these compounds show only one pyrrole-H or $-CH_2-$ peak.[1,2] The presence of one planar axial ligand whose freedom to rotate has been restricted is sufficient to break the degeneracy of the $3e(\pi)$ orbitals of Figure 1 (a, b or c, d). Such restriction in the free rotation is not unexpected in hemoglobins, myoglobins, the cytochromes, and other hemoproteins where the axial ligands are provided to the metal by side chains of the protein backbone. Two planar axial ligands (as are present in the cytochromes b_5[9,11] and b_2[9]) will split the degeneracy of the $3e(\pi)$ orbitals unless their axial ligand planes are mutually perpendicular.

Traylor and Berzinis[12] have recently demonstrated the importance of restricted rotation of an axial ligand in changing

0002-7863/80/1502-3254$01.00/0